

A compact, turnkey, narrow-bandwidth, tunable, and high-photon-flux extreme ultraviolet source

Cite as: AIP Advances **10**, 045227 (2020); <https://doi.org/10.1063/1.5133154>

Submitted: 07 February 2020 . Accepted: 01 April 2020 . Published Online: 22 April 2020

 Vinzenz Hilbert, Maxim Tschernajew, Robert Klas,  Jens Limpert, and  Jan Rothhardt

COLLECTIONS

Paper published as part of the special topic on [Chemical Physics](#), [Energy, Fluids and Plasmas](#), [Materials Science](#) and [Mathematical Physics](#)



View Online



Export Citation



CrossMark

ARTICLES YOU MAY BE INTERESTED IN

[Laboratory setup for extreme ultraviolet coherence tomography driven by a high-harmonic source](#)

Review of Scientific Instruments **90**, 113702 (2019); <https://doi.org/10.1063/1.5102129>

[Coherent narrowband light source for ultrafast photoelectron spectroscopy in the 17–31 eV photon energy range](#)

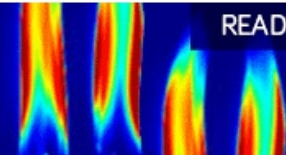
Structural Dynamics **7**, 014303 (2020); <https://doi.org/10.1063/1.5131216>

[Apparatus for soft x-ray table-top high harmonic generation](#)

Review of Scientific Instruments **89**, 083110 (2018); <https://doi.org/10.1063/1.5041498>

AIP Advances
Fluids and Plasmas Collection

READ NOW



A compact, turnkey, narrow-bandwidth, tunable, and high-photon-flux extreme ultraviolet source

Cite as: AIP Advances 10, 045227 (2020); doi: 10.1063/1.5133154

Submitted: 7 February 2020 • Accepted: 1 April 2020 •

Published Online: 22 April 2020



View Online



Export Citation



CrossMark

Vinzenz Hilbert,¹  Maxim Tschernajew,^{1,2} Robert Klas,^{1,2} Jens Limpert,^{1,2,3}  and Jan Rothhardt^{1,2,3,a)} 

AFFILIATIONS

¹Institute of Applied Physics, Friedrich-Schiller-University Jena, 07745 Jena, Germany

²Helmholtz Institute Jena, 07743 Jena, Germany

³Fraunhofer Institute for Applied Optics and Precision Engineering, 07745 Jena, Germany

^{a)}Author to whom correspondence should be addressed: j.rothhardt@gsi.de

ABSTRACT

We report on a compact high-photon-flux extreme ultraviolet (XUV) source based on high harmonic generation. A high XUV-photon flux ($>10^{13}$ photons/s) is achieved at 21.8 eV and 26.6 eV. The narrow spectral bandwidth ($\Delta E/E < 10^{-3}$) of the generated harmonics is in the range of state-of-the-art synchrotron beamlines and enables high resolution spectroscopy experiments. The robust design based on a fiber-laser system enables turnkey-controlled and even remotely controlled operation outside specialized laser laboratories, which opens the way for a variety of applications.

© 2020 Author(s). All article content, except where otherwise noted, is licensed under a Creative Commons Attribution (CC BY) license (<http://creativecommons.org/licenses/by/4.0/>). <https://doi.org/10.1063/1.5133154>

INTRODUCTION

The rapid development of table-top ultrafast laser systems over the last decade has enabled the scientific community to perform a significant number of experiments that were formerly confined to large scale facilities such as free-electron lasers (FEL) and synchrotrons.^{1–3} Among others, the development of high harmonic generation (HHG) sources opened access to photon hungry applications that require laser like extreme ultraviolet (XUV) radiation.^{4–8} In particular, the ultrashort pulse duration paired with a high photon flux is a unique property of these sources.⁹ In contrast to the typically short pulse duration and corresponding broad bandwidth of HHG sources, there are a number of applications in spectroscopy which require a narrow spectral bandwidth at XUV wavelengths. For example, material studies based on time-resolved photoelectron spectroscopy usually require a narrow bandwidth (≤ 100 meV) to discern the electronic structure and a high photon flux for reasonable acquisition times.¹⁰ In high resolution spectroscopy, similarly narrow bandwidths and high count rates are required. Here, small atomic and molecular species such as hydrogen and helium and their ionic and more exotic counterparts, antihydrogen or antiprotonic helium, are the focus of spectroscopic studies. A few of their

electrons result in a relatively simple energy level structure, which allows precise calculations based on quantum electrodynamics and subsequent comparisons with spectroscopic measurements.^{11–15} Highly charged ions provide additionally extreme conditions which challenge state-of-the-art theories.¹⁶ A few of their electrons are exposed to very strong electric and magnetic fields of the nucleus. Laser spectroscopy of their electronic structure typically requires XUV and x-ray photon energies, a narrow bandwidth, and a high photon flux.¹⁷ Meanwhile, the latest generation of high-harmonic sources appears powerful enough to enable such studies with table-top light sources, e.g., in combination with heavy ion storage rings or ion traps.¹⁸ Nevertheless, the requirements on the source are demanding, and the combination of a high photon flux and a narrow spectral bandwidth has not yet been achieved. Exceptionally narrow bandwidth harmonics ($\Delta E/E \sim 10^{-4} \dots 10^{-5}$) have already been generated by high harmonic generation with ~ 100 ps pulses.^{19,20} Unfortunately, the long pulse duration severely limited the achievable conversion efficiency, and consequently, the generated photon flux has been very low ($< 10^7$ photons/s). Recently, it has been shown that a cascaded frequency conversion scheme, namely, second harmonic generation (SHG), into the VIS subsequently followed by high harmonic generation allows for very efficient HHG

in combination with a narrow energy bandwidth.^{9,22} By decreasing the driving wavelength of the high harmonic process, the spectral bandwidth of the created harmonics is reduced due to improved phase matching. Simultaneously, the single atom response of the harmonic generation is increased, which enables higher conversion efficiencies.

So far, this approach has enabled HHG sources up to 10^{14} photons/s with a spectral bandwidth ($\Delta E/E$) of $\sim 10^{-2}$ and an average power of 1.4×10^{12} photons/s in combination with a narrow bandwidth ($\Delta E/E$) of $\sim 1.8 \times 10^{-3}$ at 26.6 eV.²¹

This article reports on a high harmonic source achieving an ultra-narrow bandwidth at the resolution limit of the employed spectrometer ($\Delta E/E = 7.5 \times 10^{-4}$) in combination with a high-XUV-photon flux in a single harmonic line ($>10^{13}$ photons/s). This unique performance is achieved by cascaded frequency conversion of a table-top ~ 300 fs infrared femtosecond fiber laser and opens up a new field of photon hungry laboratory-scale spectroscopy experiments. Moreover, the alignment-free and turnkey design of this source will enable applications outside specialized laser laboratories. For example, we envision XUV spectroscopy experiments on highly charged ions within heavy-ion storage rings and ion traps.¹⁸

SETUP

In this setup, we employ a commercially available, robust, and compact ytterbium-doped fiber laser system at a fundamental wavelength of 1030 nm as the driving system. A scheme of the experimental setup with all relevant parts is shown in Fig. 1. For the results presented here, the laser is operated at an average power of 61 W at 334 kHz for the fundamental wavelength. Subsequent frequency doubling in a 1 mm long beta barium borate (BBO) crystal yields pulse energies of 90 μ J at an average power of 30.5 W. The measured pulse duration is <300 fs. Consecutively, the beam is expanded via a telescope ($f_1 = -54$ mm, $f_2 = 217$ mm) to a beam diameter of 8 mm. For control over the beam size, a water-cooled pinhole with a fixed diameter of 8 mm is placed between the telescope lenses. An average power of 25.3 W corresponding to a pulse energy of 75 μ J is transmitted through the pinhole. Adjusting the position along the

propagation direction provides direct access to the beam size and pulse energy and enables control over optimum generation of the harmonics. Hereafter, the beam is coupled to a vacuum chamber and tightly focused ($f = 100$ mm) to a spot size of 15 μ m. A motorized nozzle with a diameter of 270 μ m is placed close to the laser focus to transport Ar gas into the focus. The generated high order harmonics are separated from the driving laser by grazing incidence plates (GIPs)²² and two 1 μ m thick aluminum filters. Subsequently, the generated EUV emission is analyzed by a flat-field grating spectrometer (1200 l/mm grating) equipped with a CCD of 2048 \times 2048 px² and a pixel size of 13.5 \times 13.5 μ m². The driving laser itself is a turnkey type system where different amplified spectra can be chosen via the SLM. The fixed position of the focusing optics and the gas jet for different driving wavelengths enables a quick and hands-off run-up phase. A run-up time as short as 30 min is, in principle, only caused by the thermalization time of the driving laser and the starting-time of the vacuum pumps at the HHG-XUV generation chamber. Note that the system presented here is fully remote controlled in the sense that the driving laser parameters, as well as the HHG optimization via the gas-jet position and the gas flow itself, can be handled remotely without a person being next to the experimental setup. For a fixed driving laser condition, the position of the gas nozzle is optimized, while the harmonic yield is monitored via the spectrometer. Correspondingly, the position of the pinhole and the backing pressure of the driving gas are adjusted for the highest HHG output in an iterative process. The optimum Ar-backing pressure is found to be 2.4 bars. For efficient retraction of the inserted Ar-gas, a second nozzle is placed on the opposite side of the Ar-inlet nozzle. This nozzle is attached to a separate vacuum pump and reduces the pressure by an order of magnitude. Correspondingly, the transmission of the created XUV is significantly increased by a factor of two. The two Al foils of 1 μ m thickness each in front of the spectrometer serve also as an attenuator of one order of magnitude per foil to prevent the saturation of the detector and to fully attenuate the residual green light.

The setup described here has already successfully been used outside a scientific laser laboratory. In this industrial-like environment (factory hall, no temperature stabilization, no additional vibration stabilization, and no cleanroom technology), the source was

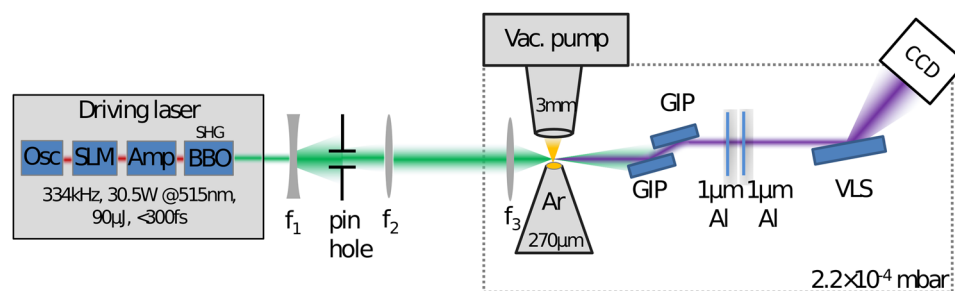


FIG. 1. Scheme of the setup. The main part of the driving laser comprises a fiber oscillator (Osc) and a spatial light modulator (SLM) to shape the amplitude and phase of the fundamental at 1030 nm. Thus, shaped pulses are further amplified (Amp) and frequency doubled (SHG) to 515 nm. Lenses f_1 and f_2 act as telescopes, where the position of the water cooled 8 mm pinhole defines the beam size. The beam is focused in vacuum via f_3 . Ar gas is introduced via a 270 μ m nozzle at the focus position and directly retracted from the vacuum chamber via an exit tube attached to a pre-vacuum pump (gray triangle). Grazing incidence plates (GIPs) separate XUV-HHG from the fundamental light. Residual fundamental and visible light is suppressed by two 1 μ m thick Al foils. A variable line space (VLS) grating separates and images the different harmonics on a CCD.

operated remotely from another building over the course of several hours.

RESULTS

Photon yield of the high harmonics

To determine the absolute photon yield, a number of optical elements in the beam path as well as absorption and beam narrowing elements have to be considered. The reflectivity of the GIP in the respective XUV wavelength range varies between 50% and 56%.^{23,24} From the measured divergence, we can infer the beam size of the XUV harmonics at the grating and account for the spatial cutting at this free aperture. A loss of 60%–70% of total intensity is determined due to cutting of the beam in the horizontal direction. The diffraction efficiency of the grating was calculated to be 4.5%–8% in the applied configuration with an incidence angle of 4°.²⁵ By spatially integrating along a Gaussian-fit to the 11th harmonic and the knowledge of the quantum efficiency of the detector, we can extract the total number of photons hitting the CCD. The measured transmission of either of the Al foils in front of the spectrometer varies between 1.2% for the 9th harmonic and 1.8% for the 11th harmonic. The residual pressure in the vacuum chambers and spectrometer is 2.2×10^{-4} mbar. Since the main contribution arises from the partial pressure of the Ar gas used for the HHG, the transmission through the vacuum system can be estimated from Ref. 26 to be ~95%. Applying all corrections to the raw data, a typical spectrum, as shown in Fig. 2, is obtained, where the number of generated photons in the 11th harmonic reaches 6.5×10^{13} photons/s and in the 9th harmonic reaches 2.0×10^{13} photons/s. Analyzing the spectral images in the non-dispersive direction yields the beam profile of the generated harmonics. Figure 3 displays the corresponding profiles for the 9th and 11th harmonic. A divergence of ± 6.2 mrad for the 9th harmonic and ± 6.3 mrad for the 11th harmonic is measured. To estimate the photon flux at a target in a potential application, one

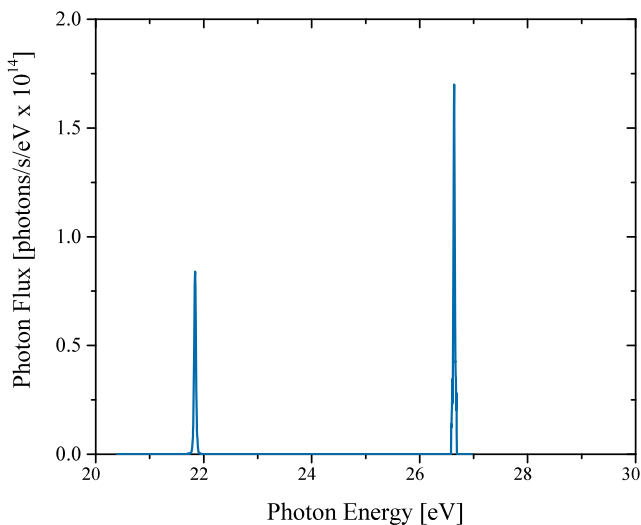


FIG. 2. Spectra of the 9th (21.5 eV, i.e., 57.6 nm) and the 11th (26.7 eV, i.e., 46.4 nm) harmonic.

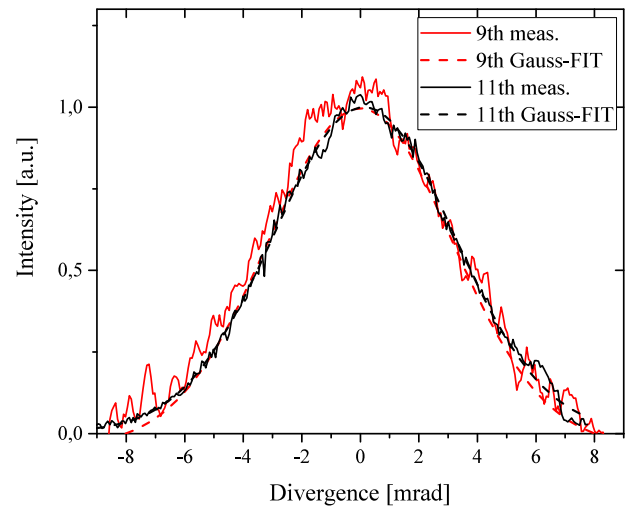


FIG. 3. Horizontal beam profile for the 9th (red) and the 11th harmonic (black).

cannot neglect the XUV transmission through a series of optical elements. Efficient filtering of the driving laser can be achieved using 2 GIPs and a 200 nm Al-filter, as described in the section “Filter transmission.” In such a case, the photon flux at the target reaches 7.8×10^{11} photons/s at the 9th harmonic and 5.1×10^{12} photons/s at the 11th harmonic.

Spectral bandwidth

The entrance-slit size of the spectrometer can be altered to merge between spectral resolution and optical throughput. To maximize the spectral resolution of the created harmonics, the spectrometer entrance opening slit, which serves as the virtual source, is set to 150 μm . A spectral bandwidth of ~20 meV [full width at half maximum (FWHM)] is determined. This corresponds to a relative energy bandwidth of $\Delta E/E = 7.5 \times 10^{-4}$. Note that the measured bandwidth in this case is only limited by the spectral resolution of the spectrometer.

Demonstration of spectral tuning

Control over the spectral properties of the driving infrared (IR) pulses is enabled via an amplitude shaper in the driving laser. Thereby, the spectrum can be patterned within the amplification bandwidth of the main amplifier.²⁷ Additional shaping of the spectral phase ensures pulse compression close to the Fourier limit. Figure 4 displays four different fundamental spectra which are shaped via the SLM to successively cover the amplification capabilities of the driving laser. For a better recognition throughout this publication, these spectra are numbered starting from longest central wavelength λ_1 , which corresponds to the lowest photon energy. The fundamental IR pulses are then frequency doubled in a 1 mm thick BBO crystal and separated from the respective fundamental radiation via dichroic mirrors. A pulse energy of 90 μJ is measured for the frequency-doubled pulses. Spectra of the SHG pulses are recorded and resemble the imprinted wavelength shift of the central wavelength of the fundamental. For all cases, we achieved sim-

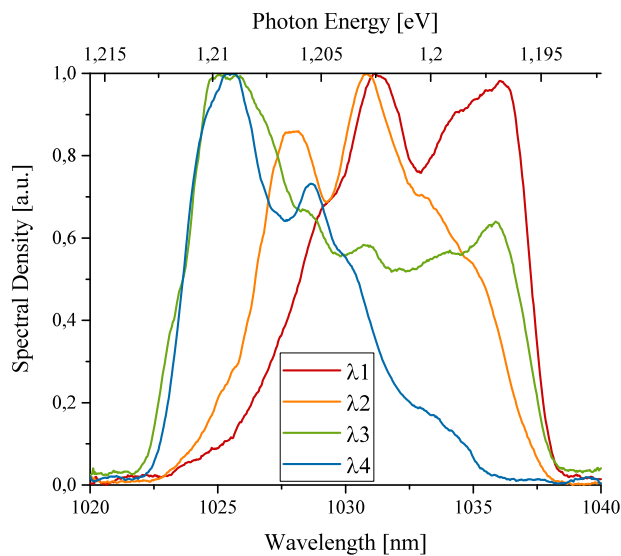


FIG. 4. IR spectra of the driving laser for different phase masks and amplitudes of the amplifier.

ilar pulse durations between 250 fs and 300 fs for the second harmonic.

To demonstrate the tunability of the XUV photon energy, XUV spectra are measured at four different amplitudes and phase masks. Figures 5 and 6 display the corresponding spectra and photon flux of the 9th and the 11th harmonic. The photon energy of the 9th harmonic can be tuned between 21.70 eV and 21.80 eV, while the photon energy of the 11th harmonic can be tuned between 26.5 eV and 26.62 eV. A comparison of the central wavelength of the harmonics to the spectral widths yields a tuning range 6 times larger than the spectral bandwidths for the 11th harmonic.

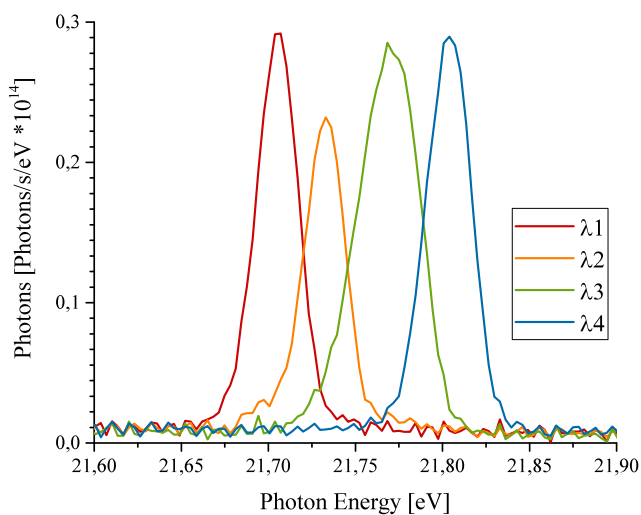


FIG. 5. Spectra of the 9th harmonic for different driving laser spectra.

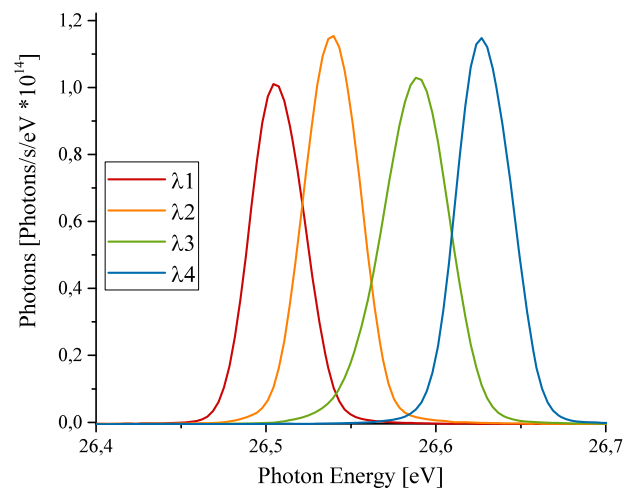


FIG. 6. Spectra of the 11th harmonic for different driving wavelengths.

Filter transmission

The XUV source described here is employed to determine the transmission of different Al filters. These ultra-thin foils are commonly used in XUV sensitive experiments where residual visible (or infrared) light is present. The visible light can be caused by various reasons, such as active pressure gauges, the driving laser, window flanges at the vacuum system, plasma glowing, and others. Typically, a few hundred nm thick Al foils are used as visible light (VIS) blocks for the XUV detectors. Transmission values for these foils in the XUV wavelength regime are usually extracted from Ref. 24. Note that the typically present surface layer of aluminum-oxide (Al_2O_3) of <5 nm thickness per surface^{28–30} has to be added manually to the data. In our experiment, a pinhole with 2 mm diameter has been set in front of the investigated foil to only illuminate the central part of the foil to avoid spatial clipping, e.g., by the filter holder. The transmission of each foil is determined from the accumulated detector counts in each harmonic with and without the particular filter in the beam. A transmission is measured for two filters with 1 μm thickness each (*Lebow Corp.*), a 200 nm filter (*Lebow Corp.*) and an ultra-flat 200 nm Al filter (*Luxel Corp.*), with a low degree of surface roughness. Figure 7 displays the measured transmission values for the 9th and the 11th harmonic. For comparison, tabulated values of the corresponding filter including surface oxidation are shown as dashed lines in the diagram. Note the striking disagreement between tabulated and measured transmission, except for the 26.5 eV transmission of the ultra-flat 200 nm Al filter. In particular, the measured transmission at 21.7 eV differs strongly from the tabulated transmission values. The ultra-flat foil holds a higher transmission for either harmonics than the standard foils. In the case of the 1 μm thick Al foils, only standard commercial foils were observed, and their measured transmission differs by an entire order of magnitude from the tabulated value at 21.7 eV, which cannot be explained by oxidization alone. Since all foils have been used in XUV experiments before and have, meanwhile, been stored during several weeks in an ambient environment, we suspect additional contamination of the foil surfaces to be the main cause of the low transmis-

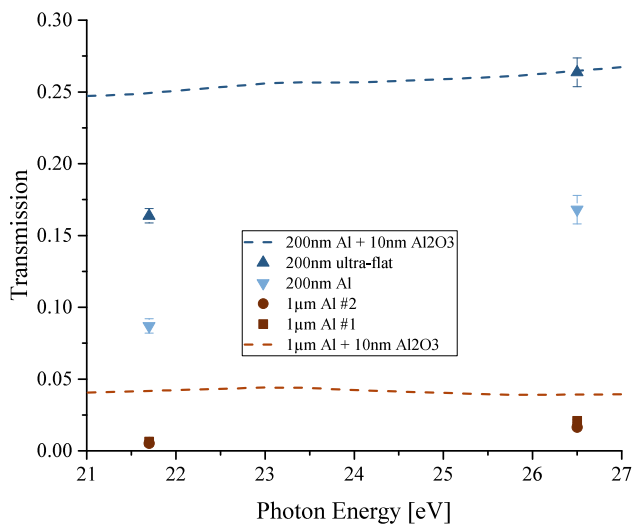


FIG. 7. Transmission of different Al filters. Single data points mark the measured transmission of the respective 9th and 11th harmonic. Dashed lines mark the tabulated values of Al foils including 5 nm surface oxidation. Like colors mark foils of the same thickness. Data for tabulated values are taken from Ref. 24.

sion. Particularly, at low photon energies, it is thus advisable to use only well-stored uncontaminated foils. In addition, this measurement shows that one cannot solely rely on tabulated transmission values but one rather has to consider the experimental history and storage conditions of a foil. Measuring the actual XUV transmission of a VIS-blocking foil throughout the experiment is strongly recommended.

CONCLUSIONS

We have set up and demonstrated a high-photon-flux XUV source based on ytterbium-doped fiber laser driven SHG–HHG. We extensively investigated the properties of the 9th and the 11th harmonic at 21 eV and 27 eV photon energies. A high photon flux of $2.0\text{--}6.5 \times 10^{13}$ photons/s together with an ultra-narrow energy bandwidth of $\Delta E/E = 7.5 \times 10^{-4}$ limited by the spectrometer resolution is measured for this source. Tuning of the central wavelength of the fundamental driving pulse comes along with the tunability of the harmonic wavelength within a range of 6-times the spectral bandwidth. In addition, the entire setup is a turnkey and remote controlled system due to the fixed setup and the easy hands-off driving laser. The combination of these features make this lab-scale XUV source a versatile tool for a number of applications that are usually carried out at synchrotron sources. We predict potential application of photoionization spectroscopy of charged ions at heavy ion storage rings, where the compact setup and high photon flux are inevitable properties.^{31,32}

ACKNOWLEDGMENTS

This research is funded by the Federal Ministry of Education and Research (BMBF), Grant No. 05P15SJFFA.

REFERENCES

- X. Qian, T. Zhang, C. Y. Ng, A. Kung, and M. Ahmed, “Two-color photoionization spectroscopy using vacuum ultraviolet synchrotron radiation and infrared optical parametric oscillator laser,” *Rev. Sci. Instrum.* **74**, 2784 (2003).
- R. L. Cavasso Filho, M. G. P. Homen, P. T. Fonseca, and A. Naves de Brito, “A synchrotron beamline for delivering high purity vacuum ultraviolet photons,” *Rev. Sci. Instrum.* **78**, 115104 (2007).
- R. Schoenlein, T. Elsaesser, K. Hollnack, Z. Huang, H. Kapteyn, M. Murnane, and M. Woerner, “Recent advances in ultrafast x-ray sources,” *Philos. Trans. R. Soc., A* **377**(2145), 20180384 (2019).
- G. Tadesse, W. Eschen, R. Klas, M. Tschernajew, F. Tuitje, M. Steinert, M. Zilk, V. Schuster, M. Zürich, T. Pertsch, C. Spielmann, J. Limpert, and J. Rothhardt, “Wavelength-scale ptychographic coherent diffractive imaging using a high-order harmonic source,” *Sci. Rep.* **9**, 735 (2019).
- R. L. Sandberg, A. Paul, D. A. Raymondson, S. Hädrich, D. M. Gaudiosi, J. Holtsnider, R. I. Tobey, O. Cohen, M. M. Murnane, H. C. Kapteyn, C. Song, J. Miao, Y. Liu, and F. Salmassi, “Lensless diffractive imaging using table-top coherent high-harmonic soft-x-ray beams,” *Phys. Rev. Lett.* **99**, 098103 (2007).
- J. Rothhardt, G. K. Tadesse, W. Eschen, and J. Limpert, “Table-top nanoscale coherent imaging with XUV light,” *J. Opt.* **20**(11), 113001 (2018).
- H. Chapman and K. A. Nugent, “Coherent lensless x-ray imaging,” *Nat. Photonics* **4**(12), 833 (2010).
- J. Miao, T. Ishikawa, I. K. Robinson, and M. M. Murnane, “Beyond crystallography: Diffractive imaging using coherent x-ray light sources,” *Science* **348**(6234), 530–535 (2015).
- H. Wang, Y. Xu, S. Ulonska, J. Robinson, P. Ranitovic, and R. Kaindl, “Bright high-repetition-rate source of narrowband extreme-ultraviolet harmonics beyond 22 eV,” *Nat. Commun.* **6**, 7459 (2015).
- T. Rohwer *et al.*, “Collapse of long-range charge order tracked by time-resolved photoemission at high momenta,” *Nature* **471**, 490–493 (2011).
- M. Herrmann *et al.*, *Phys. Rev. A* **79**, 052505 (2009).
- F. Biraben, *Eur. Phys. J.: Spec. Top.* **172**, 109–119 (2009).
- M. Hori *et al.*, *Nature* **475**, 484–488 (2011).
- S. Schippers, D. Kilcoyne, R. Phaneuf, and A. Müller, “Photoionisation of ions with synchrotron radiation: From ions in space to atoms in cages,” *Contemp. Phys.* **57**(2), 215–229 (2016).
- W. Ubachs, K. Eikema, W. Hogervorst, and P. Cacciani, “Narrow-band tunable extreme-ultraviolet laser source for lifetime measurements and precision spectroscopy,” *J. Opt. Soc. Am. B* **14**, 2469–2476 (1997).
- J. Gillaspay, “Highly charged ions,” *J. Phys. B* **34**, R93 (2001).
- S. Epp, J. López-Urrutia, G. Brenner, V. Mäckel, P. Mokler, R. Treusch, M. Kuhlmann, M. Yurkov, J. Feldhaus, J. Schneider, M. Wellhöfer, M. Martins, W. Wurth, and J. Ullrich, “Soft x-ray laser spectroscopy on trapped highly charged ions at FLASH,” *Phys. Rev. Lett.* **98**, 183001 (2007).
- J. Rothhardt, S. Hädrich, S. Demmler, M. Krebs, D. Winters, T. Kühl, T. Stöhler, J. Limpert, and A. Tünnermann, “Prospects for laser spectroscopy of highly charged ions with high-harmonic XUV and soft x-ray sources,” *Phys. Scr.* **T166**, 14030 (2015).
- F. Brandi, D. Neshev, and W. Ubachs, “High-order harmonic generation yielding tunable extreme-ultraviolet radiation of high spectral purity,” *Phys. Rev. Lett.* **91**, 163901 (2003).
- C. Lyngå, F. Oessler, T. Metz, and J. Larsson, “A laser system providing tunable, narrow-band radiation from 35 nm to 2 μm,” *Appl. Phys. B* **72**, 913–920 (2001).
- R. Klas, S. Demmler, M. Tschernajew, S. Hädrich, Y. Shamir, A. Tünnermann, J. Rothhardt, and J. Limpert, “Table-top milliwatt-class extreme ultraviolet high harmonic light source,” *Optica* **3**, 1167–1170 (2016).
- O. Pronin, V. Pervak, E. Fill, J. Rauschenberger, F. Krausz, and A. Apolonski, “Ultrabroadband efficient intracavity XUV output coupler,” *Opt. Express* **19**(11), 10232–10240 (2011).

- ²³R. Klas, A. Kirsche, M. Tschernajew, J. Rothhardt, and J. Limpert, “Annular beam driven high harmonic generation for high flux coherent XUV and soft x-ray radiation,” *Opt. Express* **26**(15), 19318–19327 (2018).
- ²⁴B. L. Henke, E. M. Gullikson, and J. C. Davis, “X-ray interactions: Photoabsorption, scattering, transmission, and reflection at $E = 50\text{--}30,000$ eV, $Z = 1\text{--}92$,” *At. Data Nucl. Data Tables* **54**(2), 181–342 (1993).
- ²⁵A. Haage, “Development of an XUV Spectrometer for diagnostics of high harmonic radiation pulses generated in a gas jet array,” Diploma thesis, University of Hamburg, 2012.
- ²⁶See www.henke.lbl.gov for transmission of XUV-light through different materials.
- ²⁷A. Weiner, “Femtosecond pulse shaping using spatial light modulators,” *Rev. Sci. Instrum.* **71**, 1929 (2000).
- ²⁸C. Chen, S. Splinter, T. Do, and N. S. McIntyre, “Measurement of oxide film growth on Mg and Al surfaces over extended periods using XPS,” *Surf. Sci.* **382**, L652–L657 (1997).
- ²⁹J. Zähr, S. Oswald, M. Türpe, H. Ullrich, and U. Füssel, “Characterisation of oxide and hydroxide layers on technical aluminum materials using XPS,” *Vacuum* **86**, 1216–1219 (2012).
- ³⁰T. Do, S. Splinter, C. Chen, and N. S. McIntyre, “The oxidation kinetics of Mg and Al surfaces studied by AES and XPS,” *Surf. Sci.* **387**, 192–198 (1997).
- ³¹M. Lestinsky *et al.*, “Physics book: CRYRING@ESR,” *Eur. Phys. J.: Spec. Top.* **225**, 797–882 (2016).
- ³²J. Rothhardt, M. Bilal, R. Beerwerth, A. Volotka, V. Hilbert, T. Stöhlker, S. Fritzsche, and J. Limpert, “Lifetime measurements of ultra-short-lived excited states in Be-like ions,” *X-Ray Spectrom.* **49**, 165–168 (2020).